Physics Letters B 745 (2015) 58–63

Contents lists available at ScienceDirect

Physics Letters B

www.elsevier.com/locate/physletb

Constraining interactions mediated by axion-like particles with ultracold neutrons

S. Afach [a,b,c], G. Ban [d], G. Bison [b], K. Bodek [e], M. Burghoff [f], M. Daum [b], M. Fertl [a,b,1], B. Franke [a,b,*,2], Z.D. Grujić [g], V. Hélaine [b,d], M. Kasprzak [g], Y. Kermaïdic [h], K. Kirch [a,b], P. Knowles [g,3], H.-C. Koch [g,i], S. Komposch [a,b], A. Kozela [j], J. Krempel [a], B. Lauss [b,*], T. Lefort [d], Y. Lemière [d], A. Mtchedlishvili [b], O. Naviliat-Cuncic [d,4], F.M. Piegsa [a], G. Pignol [h], P.N. Prashanth [k], G. Quéméner [d], D. Rebreyend [h], D. Ries [a,b], S. Roccia [l,*], P. Schmidt-Wellenburg [b], A. Schnabel [f], N. Severijns [k], J. Voigt [f], A. Weis [g], G. Wyszynski [a,e], J. Zejma [e], J. Zenner [a], G. Zsigmond [b]

[a] ETH Zürich, Institute for Particle Physics, CH-8093 Zürich, Switzerland
[b] Paul Scherrer Institute (PSI), CH-5232 Villigen-PSI, Switzerland
[c] Hans Berger Department of Neurology, Jena University Hospital, D-07747 Jena, Germany
[d] LPC Caen, ENSICAEN, Université de Caen, CNRS/IN2P3, Caen, France
[e] Marian Smoluchowski Institute of Physics, Jagiellonian University, 30-059 Cracow, Poland
[f] Physikalisch Technische Bundesanstalt, D-10587 Berlin, Germany
[g] Physics Department, University of Fribourg, CH-1700 Fribourg, Switzerland
[h] LPSC, Université Grenoble Alpes, CNRS/IN2P3, Grenoble, France
[i] Institut für Physik, Johannes–Gutenberg–Universität, D-55128 Mainz, Germany
[j] Henryk Niedwodniczański Institute for Nuclear Physics, 31-342 Cracow, Poland
[k] Instituut voor Kern–en Stralingsfysica, University of Leuven, B-3001 Leuven, Belgium
[l] CSNSM, Université Paris Sud, CNRS/IN2P3, Orsay Campus, France

ARTICLE INFO

Article history:
Received 9 December 2014
Received in revised form 30 March 2015
Accepted 14 April 2015
Available online 20 April 2015
Editor: M. Doser

Keywords:
CP violation
Short range spin-dependent interaction
Axion
Axion-like particle
Ultracold neutrons
Neutron electric dipole moment

ABSTRACT

We report a new limit on a possible short range spin-dependent interaction from the precise measurement of the ratio of Larmor precession frequencies of stored ultracold neutrons and ^{199}Hg atoms confined in the same volume. The measurement was performed in a $\sim$1 μT vertical magnetic holding field with the apparatus searching for a permanent electric dipole moment of the neutron at the Paul Scherrer Institute. A possible coupling between freely precessing polarized neutron spins and unpolarized nucleons of the wall material can be investigated by searching for a tiny change of the precession frequencies of neutron and mercury spins. Such a frequency change can be interpreted as a consequence of a short range spin-dependent interaction that could possibly be mediated by axions or axion-like particles. The interaction strength is proportional to the CP violating product of scalar and pseudoscalar coupling constants $g_S g_P$. Our result confirms limits from complementary experiments with spin-polarized nuclei in a model-independent way. Limits from other neutron experiments are improved by up to two orders of magnitude in the interaction range of $10^{-6} < \lambda < 10^{-4}$ m.

1. Introduction

We present an interpretation of our recent measurement of the ratio γ_n/γ_{Hg} of the neutron and ^{199}Hg magnetic moments [1] in terms of the strength of a possible short range spin-dependent neutron–nucleon interaction. This ratio was inferred from a comparison of the simultaneously recorded Larmor precession frequencies of the two species contained in the same storage volume. The

* Corresponding author.
E-mail addresses: beatrice.franke@mpq.mpg.de (B. Franke), bernhard.lauss@psi.ch (B. Lauss), stephanie.roccia@csnsm.in2p3.fr (S. Roccia).
[1] Now at University of Washington, Seattle WA, USA.
[2] Now at Max-Planck-Institute of Quantum Optics, Garching, Germany.
[3] Now at LogrusData, Vienna, Austria.
[4] Now at Michigan State University, East-Lansing, USA.

http://dx.doi.org/10.1016/j.physletb.2015.04.024

measurement was performed using the apparatus dedicated to the search for the neutron electric dipole moment (nEDM) [2] by the nEDM Collaboration at the source for ultracold neutrons [3] of the Paul Scherrer Institute, Switzerland.

In the central storage vessel of the apparatus, the spins of the neutrons and mercury atoms are made to precess simultaneously in the same volume. The ratio

$$R = \frac{f_{\mathrm{n}}}{f_{\mathrm{Hg}}} \tag{1}$$

constitutes a sensitive tool for the control of systematic effects during the measurement of the nEDM. By correcting R properly for known differences of the Larmor precession of the two species neutrons and ^{199}Hg, respectively, the ratio of magnetic moments $\gamma_{\mathrm{n}}/\gamma_{\mathrm{Hg}}$ can be extracted. A data set of R taken in 2012 was independently analysed in [1] and in [4], where we additionally examined its sensitivity to hypothetical short range spin-dependent interactions. Possible force mediators are axions, or axion-like particles and the interaction strength is proportional to the product of scalar and pseudoscalar coupling constants $g_S g_P$. It has been proposed in [5,6] to use an nEDM apparatus for the investigation of such a force.

A motivation to search for an interaction involving $g_S g_P$ is given in Section 2. The influence of a short range spin-dependent interaction on the observable R is explained and derived in Section 3, where additionally some related details about the experiment are shown. Our result is compared to other current limits on the product $g_S g_P$ in Section 4.

2. Motivation

The investigation of CP violating processes is a major line of research in particle physics. In contrast to the weak interaction, there is so far no evidence that the strong interaction violates CP symmetry. The non-observation of an nEDM at current sensitivity levels constrains the CP violating term (θ-*term*) in the Lagrangian of the strong interaction to be nine orders of magnitude smaller than naturally expected [7]. This fact is known as *the strong CP problem* and a solution to it was proposed in [8], where the spontaneously broken Peccei–Quinn symmetry was introduced.

A new pseudoscalar boson emerges from this symmetry, the axion [9,10]. An intrinsic feature of the Peccei–Quinn model is a fixed relation between mass and interaction strength of the axion. The originally assumed symmetry breaking scale (corresponding to the electroweak scale) was ruled out, leaving only higher energy scales possible. For the axion one thus expects a small mass and a feeble interaction with other particles. The possible mass of the axion is constrained by cosmology and astro-particle physics measurements to the so-called *axion window* [11].

A short range spin-dependent interaction which could be mediated by an axion was proposed in [12]. There, three classes of interactions were presented, involving either g_S^2-, $g_S g_P$-, or g_P^2-couplings, whereas $g_S g_P$-couplings are considered of particular interest, since they violate CP symmetry. A $g_S g_P$-coupling diagram is shown in Fig. 1(a) and takes place between an unpolarized particle Ψ (where *unpolarized* means randomly polarized with respect to any quantization axis) and a polarized particle $\Phi^\diamond$. The symbol $^\diamond$ is used to denote properties of the particle interacting at the pseudoscalar vertex with a strength proportional to the coupling constant $g_P^\diamond$ of the particle $\Phi^\diamond$. The potential caused by such a $g_S g_P^\diamond$-coupling between an unpolarized particle and a polarized particle with mass $m^\diamond$ and spin $\boldsymbol{\sigma}^\diamond$ is derived as [12]:

$$V(\boldsymbol{r}) = g_S g_P^\diamond \frac{(\hbar c)^2}{8\pi m^\diamond c^2} (\hat{\boldsymbol{\sigma}}^\diamond \cdot \hat{\boldsymbol{r}}) \left(\frac{1}{r\lambda} + \frac{1}{r^2}\right) e^{-r/\lambda}, \tag{2}$$

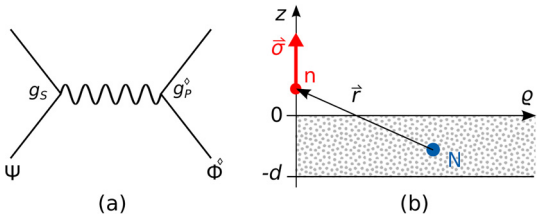

Fig. 1. (a) Interaction diagram of a scalar-pseudoscalar coupling between particles Ψ and $\Phi^\diamond$. Ψ is unpolarized and interacts at the scalar vertex with the coupling constant g_S, whereas $\Phi^\diamond$ is polarized and interacts at the pseudoscalar vertex with the coupling constant $g_P^\diamond$. The total interaction strength is proportional to the product $g_S g_P^\diamond$. (b) A polarized neutron n with spin $\boldsymbol{\sigma}$ interacts with an unpolarized nucleon N at distance $\boldsymbol{r}$ within bulk matter shaped as a plate of thickness d. A view of the ϱ–z plane in a cylindrical coordinate system (ϱ, ϕ, z) is shown.

where $\hat{\boldsymbol{\sigma}}^\diamond$ is the unit vector of the spin, $\hat{\boldsymbol{r}}$ is the unit vector along the distance $\boldsymbol{r}$ between the particles, and λ the interaction range. The product $(\hat{\boldsymbol{\sigma}}^\diamond \cdot \hat{\boldsymbol{r}})$ also violates parity P and time reversal symmetry T.

$g_S g_P$-couplings can also be mediated by other hypothetical spin-zero particles which are generic to the axion and usually referred to as axion-like particles. However, for these generic bosons no relation between mass and interaction strength is given, as compared to the genuine axion. The origin of such particles can be symmetries other than Peccei–Quinn symmetry, which are broken at very high energies and often postulated in theories beyond the Standard Model of particle physics, such as e.g. String Theory. Thus, both axions and axion-like particles, are intriguing dark matter candidates and beyond Standard Model physics probes [13–15].

However, due to the non-observation of the nEDM a short range spin-dependent interaction mediated by an axion is constrained to $g_S g_P < 10^{-40} \ldots 10^{-34}$ [16]. On the other hand, if the force is mediated by an axion-like particle, g_S and g_P are not related to a specific symmetry breaking scale. Thus, no significant constraint (i.e. comparable to experimental sensitivity ranges) on $g_S g_P$ can be deduced from current EDM limits [16] for the case of a generic boson being the interaction mediator.

Our measurement with ultracold neutrons is particularly sensitive to axion-like particles with a mass in the range of roughly 10 meV to 100 meV coupling to fermions. It also matches the mass range targeted by helioscopes such as CAST [17] which would be sensitive to axion-like particles coupling to photons.

3. The measurement with the nEDM apparatus

The experiment is performed by confining ultracold neutrons (UCN) of energies below 160 neV [18,19] in a cylindrical storage chamber with vertical axis at the center of the nEDM apparatus. The dimensions of the storage chamber and some specific features are shown in Fig. 2. A homogeneous vertical magnetic holding field of $\sim$1 µT is applied with a $\cos\theta$-coil wound around the horizontally cylindrical vacuum tank. This vacuum tank is enclosed by a four-layer magnetic shielding [20] and an active magnetic field stabilisation system for the external magnetic field [21].

Spin-polarized UCN are filled into the storage chamber approximately every 340 s where they precess freely for 180 s during the described measurements. The precession frequency is inferred using Ramsey's method [2]. The spins of polarized ^{199}Hg atoms precess simultaneously in the same volume allowing to correct the Larmor precession frequency of the neutrons for potential, small magnetic field fluctuations which can occur inside the four-layer magnetic shielding made of µ-metal.

We search for a signature of a spin-dependent interaction between polarized particles inside the storage chamber and the unpolarized wall of this chamber. This interaction can be described

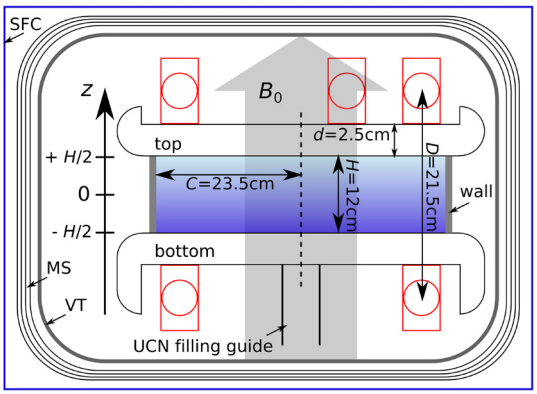

Fig. 2. Vertical cut view of the UCN storage chamber with important parts schematically indicated (not to scale). The big grey arrow indicates the main magnetic holding field B_0. The blue shaded region is the inside of the chamber and indicates the inhomogeneous UCN density distribution. The red shapes depict Cs magnetometers [22] which are mounted above and below the storage chamber: four on top and seven at the bottom. These consist of a Cs-vapour filled glass bulb inside a shielded housing and serve to measure the vertical main magnetic field B_0 and also vertical magnetic field gradients G. The measures are the thickness d of the top and bottom plates of the vessel (coated with diamond-like carbon for improved UCN storage properties [18]), distance D between top and bottom Cs magnetometers, height H of the vessel, and radius C of the vessel. UCN are filled through a guide from below. The lateral wall of the vessel is a polystyrene ring with a deuterated coating for improved UCN storage properties [19]. The vacuum tank (VT) of the apparatus is enclosed by a four-layer magnetic shielding (MS) made from μ-metal [20] and a surrounding field compensation (SFC) which actively stabilises the external magnetic field [21]. (For interpretation of the references to color in this figure legend, the reader is referred to the web version of this article.)

by the potential of Eq. (2) and an example is shown in Fig. 1(b). Integrating the interaction over all the nucleons present in uniform bulk matter results in an effective field normal to the surface.

Since the potential is spin-dependent, it can also be regarded as a pseudomagnetic field b which can affect the Larmor frequency of precessing spins. For a symmetric setup with identical material for the bottom and top of the storage vessel, the field at the vessel surfaces points in opposite directions. Therefore, we expect no shift in the Larmor frequency of the Hg atoms which sample the volume homogeneously. However, UCNs have such low energies that they are significantly affected by gravity and their density increases towards the bottom of the storage vessel. Thus, the vessel is inhomogeneously sampled and the effect of a pseudomagnetic field at the bottom of the chamber will not cancel out completely. Depending on the sign of the vertical magnetic field, the precession frequency of the UCN spins will be increased or decreased. Consequently, R will be shifted by a constant with opposite sign for the upward or downward oriented magnetic holding field B_0:

$$R^{\uparrow\downarrow} = \frac{\gamma_n}{\gamma_{Hg}}\left(1 \pm \frac{b}{B_0}\right), \tag{3}$$

where the $\pm$ sign applies to the upward/downward oriented magnetic holding field, respectively.

3.1. Derivation of the pseudomagnetic field

Integrating the potential given in Eq. (2) over bulk matter, e.g. a plate of thickness d, radius C, and nucleon number density N, results in a total potential V_{tot} at height z above the surface of the plate (cylindrical coordinates $\boldsymbol{r} = (\varrho, \phi, z)$ are used) [4]:

$$V_{tot}(z) = \int_0^{-d}\int_0^{2\pi}\int_0^{C} NV(\boldsymbol{r})\ \varrho\, \mathrm{d}\varrho\, \mathrm{d}\phi\, \mathrm{d}z \tag{4}$$

$$= g_S g_P^{\diamond} \frac{\hbar^2 N\lambda}{4m^{\diamond}}\left(e^{-\frac{z}{\lambda}} - e^{-\frac{z+d}{\lambda}} - e^{-\frac{\sqrt{C^2+z^2}}{\lambda}} + e^{-\frac{\sqrt{C^2+(z+d)^2}}{\lambda}}\right) \tag{5}$$

$$\approx g_S g_P^{\diamond} \frac{\hbar^2 N\lambda}{4m^{\diamond}}\left(1 - e^{-d/\lambda}\right)e^{-z/\lambda}. \tag{6}$$

The approximation from Eq. (5) to (6) neglects the third and fourth terms in the round brackets and is well justified due to the dimensions of the chamber ($d \ll C$), and the range of interest of λ and z ($\lambda, z \ll C$). It also corresponds to simplifying the integration over the radial component ϱ to an infinite plane.

The pseudomagnetic field b normal to the surface can be written as a function of height z:

$$b(z) = \frac{2V_{tot}(z)}{\gamma^{\diamond}\hbar} \approx g_S g_P^{\diamond} \frac{\hbar\lambda N}{2\gamma^{\diamond} m^{\diamond}}\left(1 - e^{-d/\lambda}\right)\left(e^{-z/\lambda}\right), \tag{7}$$

where $\gamma^{\diamond}$ is the gyromagnetic ratio of the polarized particle. This result agrees with the one derived in [5].

In order to calculate the field present in the nEDM setup b_{nedm}, both the bottom and the top of the storage vessel have to be taken into account. The vessel's inner horizontal surfaces are perpendicular to $\boldsymbol{z}$, with the bottom surface at $z = -H/2$ and the top surface at $z = +H/2$, as shown in Fig. 2. Using Eq. (7) one finds

$$b_{nedm}(z) = b_{bottom}\, e^{-\frac{z+H/2}{\lambda}} - b_{top}\, e^{-\frac{-z+H/2}{\lambda}}. \tag{8}$$

Because of their inhomogeneous density distribution $\rho(z)$, the UCN experience an effective field given by

$$b_{UCN} = \int_{-\frac{H}{2}}^{\frac{H}{2}} b_{nedm}(z)\rho(z)\ \mathrm{d}z. \tag{9}$$

The first order estimate for the UCN density distribution is

$$\rho(z) = \frac{1}{H}\left(1 + \frac{12h}{H^2}z\right), \tag{10}$$

where $h = -2.35(5)$ mm is the measured center-of-mass offset between UCN and Hg atom distributions (see also Section 3.2).

Since the pseudomagnetic field is expected to be of short interaction range λ given by the limits which have already been imposed on $g_S g_P$, the UCN density distribution can be approximated with a constant value within a distance $\sim\lambda$ to the bottom and top surfaces. As a consequence, Eq. (9) can be simplified in the following way:

$$b_{UCN} \approx \int_{-\frac{H}{2}}^{\frac{H}{2}} \left(\rho_{bottom}\, b_{bottom}\, e^{-\frac{z+H/2}{\lambda}} - \rho_{top}\, b_{top}\, e^{-\frac{-z+H/2}{\lambda}}\right)\mathrm{d}z, \tag{11}$$

where $\rho_{bottom} = \rho(-H/2)$ and $\rho_{top} = \rho(+H/2)$. Thus the integral can be solved analytically and the scalar and pseudoscalar coupling constants can be isolated as follows:

$$g_S g_P^{\diamond} = b_{UCN} \frac{H^2\gamma^{\diamond} m^{\diamond}}{6\hbar h N\lambda^2}\left(1 - e^{-H/\lambda}\right)^{-1}\left(1 - e^{-d/\lambda}\right)^{-1}. \tag{12}$$

The bottom and top of the UCN storage vessel are made of aluminum and have a thickness of $d = 2.5$ cm each. We use $N \equiv N_{Al} = 1.62 \cdot 10^{24}\,\mathrm{cm}^{-3}$ and $\gamma^{\diamond} \equiv \gamma_n = 2\pi \cdot 29.1646943\,\mathrm{MHz/T}$ [23]. The surface of the aluminum plates is coated with diamond-like carbon in order to improve neutron storage properties. The coating thickness is below 3 μm and the density of diamond-like carbon

is similar to that of aluminum. Thus the coating is disregarded in the calculation but for the fact that we restrict the validity of our derived limit to $\lambda > 1\,\mu m$.

The center-of-mass offset h contributes to the denominator of Eq. (12) and depends on the energy spectrum of the UCN. Hence, a change in the energy spectrum, or also a different vessel height H, will influence the sensitivity of our apparatus to a pseudomagnetic field.

3.2. Details on the measurement of the ratio R and the center-of-mass offset h

In [1], the measurement of R and its experimental setup are thoroughly described. Here we briefly recapitulate selected aspects of the experiment and related systematics relevant to our measurement.

Taking into account systematic shifts on the UCN or mercury spin precession frequency, the ratio R can be rewritten as:

$$R = \frac{f_n}{f_{Hg}} = \frac{\gamma_n}{\gamma_{Hg}}\left(1 + \delta_{Grav} + \delta_{Trans} + \delta_{Light} + \delta_{Earth}\right). \tag{13}$$

A linear, G-dependent fit of the form $x + Gy$, where $G = \partial B/\partial z$ is the vertical magnetic field gradient, was performed to the data listed in Table 2 of [1]. The first two terms in Eq. (13) constitute the terms of the fit. The other terms shift the constant fit parameter and add to the systematic error. The different contributions to Eq. (13) are discussed in the following.

Firstly we want to focus on the shifts δ_{Grav} and δ_{Trans} which are both related to the very low kinetic energies of the UCN.

The gravitation-induced systematic effect is described at first order by

$$\delta^{\uparrow\downarrow}_{Grav} = \pm\frac{h}{B_0}G, \tag{14}$$

where the plus-sign refers to ${B_0}^{\uparrow}$ and the minus-sign to ${B_0}^{\downarrow}$. Eq. (14) is derived assuming a UCN density distribution as given in Eq. (10) and thus the common slope in both equations corresponds to the center-of-mass offset h of the UCN. The linear gradient dependence is assumed to hold for small G. Measuring R as a function of varying vertical magnetic field gradients enables us extract the center-of-mass offset h from the slope of R vs. G.

Two correction coils (wound as saddle coils on top and bottom of the vacuum tank) were powered in an anti-Helmholtz configuration to superimpose a vertical magnetic field gradient to B_0. A measurement of the magnitude of G is provided by cesium magnetometers [22] which are located above and below the UCN storage vessel (see Fig. 2). A second order polynomial parametrization of the magnetic field is used to extract G from the magnetometers' readings and their positions.

The systematic effect due to possible transverse components of B_0 reads

$$\delta^{\uparrow\downarrow}_{Trans} = \frac{\langle {B_\perp}^2\rangle^{\uparrow\downarrow}}{2{B_0}^2}, \tag{15}$$

where $\langle {B_\perp}^2\rangle^{\uparrow\downarrow}$ is the storage chamber volume average of transverse magnetic field components $B_\perp$ for the case of the main magnetic field B_0 being oriented upwards or downwards, respectively. This correction results from the fact that, given by their low velocities, the neutrons are in the adiabatic regime (Larmor frequency > wall collision rate) and their precession frequency is proportional to the average magnetic field modulus $f_n \propto \langle|\boldsymbol{B}|\rangle$. Whereas for the mercury atoms with thermal velocities (Larmor frequency < wall collision rate), $f_{Hg} \propto |\langle \boldsymbol{B}\rangle|$.

Table 1
Relative contributions to the overall error listed by the effect which contributes to the magnetic field.

Effect	${B_0}^{\uparrow}$	${B_0}^{\downarrow}$
Statistics	$\pm 0.5 \cdot 10^{-6}$	$\pm 0.5 \cdot 10^{-6}$
Gravitational shift	$(-8.9 \pm 2.3) \cdot 10^{-6}$	$(-1.8 \pm 2.7) \cdot 10^{-6}$
Transverse shift	$(3.7 \pm 0.8) \cdot 10^{-6}$	$(3.0 \pm 1.2) \cdot 10^{-6}$
Light shift	$(1.3 \pm 0.7) \cdot 10^{-6}$	$(0.8 \pm 0.6) \cdot 10^{-6}$
Earth rotation shift	$-5.3 \cdot 10^{-6}$	$+5.3 \cdot 10^{-6}$

A magnetic field mapping was performed inside the vacuum tank with a sophisticated non-magnetic robot using a custom-made high sensitivity triaxial fluxgate magnetometer. The volume of the precession chamber has been mapped. The following results for the two magnetic field orientations were obtained:

$$\left\langle {B_\perp}^2\right\rangle^{\uparrow} = (2.1 \pm 0.5)\,\mathrm{nT}^2; \quad \left\langle {B_\perp}^2\right\rangle^{\downarrow} = (1.7 \pm 0.7)\,\mathrm{nT}^2. \tag{16}$$

These numbers have to be regarded in relation to the absolute value of the magnetic field of $\sim 1\,\mu T$. Comparing the two values for $\uparrow$ and $\downarrow$ with each other also demonstrates how well a polarity change of B_0 resembles a perfect inversion of the magnetic field.

δ_{Light} results from a shift of f_{Hg} due to light-intensity-dependent effects during the optical read-out of the mercury precession frequency as explained in [24]. The corresponding correction factors are given in Table 1 (fourth row).

The remaining δ_{Earth} is a consequence of the Earth being a rotating frame of reference. In this context it is of particular interest that neutrons and mercury atoms have different signs of their gyromagnetic ratios, i.e. they precess in different directions with respect to the magnetic field. This can be corrected for by applying the terms in Table 1 (fifth row).

All systematic error contributions are summarized in the error budget for the measurement of the ratio R in Table 1. We can derive two independent values for R using the data for ${B_0}^{\uparrow}$ and ${B_0}^{\downarrow}$, respectively and the error contributions from Table 1:

$$R^{\uparrow} = 3.8424583(26) \tag{17}$$

$$R^{\downarrow} = 3.8424562(30). \tag{18}$$

From the difference of $R^{\uparrow}$ and $R^{\downarrow}$ (as given in Eq. (3)) and the sum $R^{\uparrow} + R^{\downarrow} = 2\gamma_n/\gamma_{Hg}$ we can extract

$$b_{UCN} = \frac{\left(R^{\uparrow} - R^{\downarrow}\right)}{\left(R^{\uparrow} + R^{\downarrow}\right)}B_0 = (0.28 \pm 0.53)\,\mathrm{pT}. \tag{19}$$

4. Result and comparison to other experiments

Using Eq. (12), the measured pseudomagnetic field b_{UCN} can be converted to a 95% confidence level limit on $g_S g_P$

$$g_S g_P \lambda^2 < 2.2 \cdot 10^{-27}\,\mathrm{m}^2 \tag{20}$$

for $1\,\mu m < \lambda < 5\,mm$. At the upper end of this range, the last factor in Eq. (12) departs from ~ 1 and the relation $g_S g_P \propto 1/\lambda^2$ is not fulfilled anymore. As a consequence the sensitivity of our experiment to $g_S g_P$ decreases which results in a flattening of the limit in the $g_S g_P$ vs. λ-plane (see Fig. 3). The lower end of this range is constrained by the wavelength of ultracold neutrons and affected by surface properties such as coating, roughness, etc.

Since we investigated an interaction between unpolarized nucleons and polarized neutrons, we can state that we probed the scalar coupling constant generally valid for nucleons $g_S \equiv g_S^N$ and the pseudoscalar coupling constant specific to the neutron $g_P^{\circ} \equiv g_P^n$.

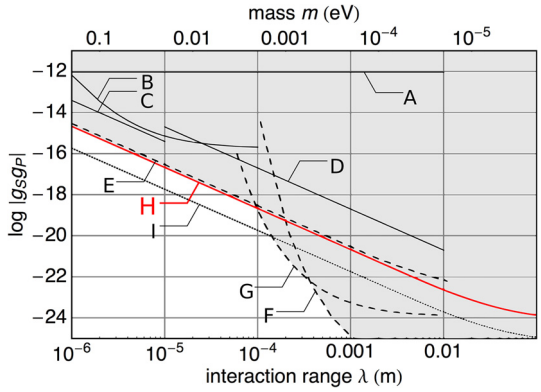

Fig. 3. Overview of current limits on the product of scalar and pseudoscalar coupling constants $g_S g_P$ as function of the interaction range λ of a short range spin-dependent force at 95% confidence level. On the top, the corresponding mass range of the mediating particle, i.e. axion or axion-like particle, is shown. The shaded region is excluded by different experiments. Solid line limits were obtained using cold or ultracold neutrons. Dashed line limits were obtained using ^{3}He, ^{129}Xe, or ^{131}Xe precession experiments. A [30]; B [31], assuming an attractive interaction; C [32]; D [6]; E [29]; F [26]; G [27]; and H (red in the web version) this work. The line I (dotted) depicts the achievable limit by a simple modification of our apparatus (see text).

Fig. 3 compares our limit on $g_S g_P$ to results from other experiments. It covers the interaction range of $1\,\mu\text{m} < \lambda < 0.1\,\text{m}$, which is not yet strongly excluded by astrophysical or cosmological constraints.

Experiments using free neutrons are depicted by solid lines. Experiments with precessing atoms, such as e.g. ^{3}He, ^{129}Xe, or ^{131}Xe, are depicted by dashed lines. According to the Schmidt Model [25], polarized atoms of odd isotopes (with one unpaired nucleon) can roughly be considered as a probe for the magnetic properties of this unpaired nucleon, regardless of the other constituents of the nucleus. Under this assumption, both types of experiments probe $g_S^{\text{N}} g_P^{\text{n}}$. While these approaches are complementary, the direct neutron measurements are model independent. The most stringent limits for $\lambda > 10^{-4}\,\text{m}$ have been imposed recently in [26] and [27] (curves labelled F and G in Fig. 3, respectively) which improved the recent limits from [28]. For shorter interaction ranges, the most stringent limit was given in [29] (E), where relaxation of spin polarized ^{3}He gas was investigated. This limit has been model independently confirmed and slightly improved by the measurements presented in this work (H). Limits derived from experiments with neutrons (A,B,C,D) [30–32,6] were improved by one order of magnitude for $\lambda < 10^{-5}$ and by two orders of magnitude for $\lambda > 10^{-5}$. In [33] a stronger but indirect limit on $g_S g_P$ was imposed by combining laboratory results with stellar energy loss arguments. Such limits might be reached with dedicated future laboratory searches e.g. proposed in [34].

Already our present result constitutes a new direct limit on $g_S g_P$. Replacing in our experiment the central vessel bottom and top with copper, a material with higher density and good UCN reflecting surface properties, would result in a sensitivity gain of $\sim$3, corresponding to the density ratio between copper and aluminum. Replacing either only the bottom or top would create a true asymmetric potential and increase the sensitivity by one order of magnitude [4]. The consequently achievable limit depicted by the dotted curve (I) in Fig. 3 would be an important contribution to reduce the allowed parameter spaces of beyond Standard Model theories.

Acknowledgements

We are grateful to the PSI staff (the accelerator operating team and the BSQ group) for providing excellent running conditions and acknowledge the outstanding support of M. Meier and F. Burri. Support by the Swiss National Science Foundation Projects 200020-144473 (PSI), 200021-126562 (PSI), 200020-149211 (ETH) and 200020-140421 (Fribourg) is gratefully acknowledged. The LPC Caen and the LPSC Grenoble acknowledge the support of the French Agence Nationale de la Recherche (ANR) under reference ANR-09–BLAN-0046. The Polish collaborators acknowledge the National Science center, Poland, for the grant No. UMO-2012/04/M/ST2/00556 and the support by the Foundation for Polish Science – MPD program, co-financed by the European Union within the European Regional Development Fund. This work was partly supported by the Fund for Scientific Research Flanders (FWO), and Project GOA/2010/10 of the KU Leuven. The original apparatus was funded by grants from the UK's PPARC.

References

[1] S. Afach, C.A. Baker, G. Ban, et al., Phys. Lett. B 739 (2014) 128, http://dx.doi.org/10.1016/j.physletb.2014.10.046.
[2] C.A. Baker, G. Ban, K. Bodek, et al., Phys. Proc. 17 (2011) 159, http://dx.doi.org/10.1016/j.phpro.2011.06.032.
[3] B. Lauss, Hyperfine Interact. 211 (2012) 21, http://dx.doi.org/10.1007/s10751-012-0578-7.
[4] B. Franke, PhD thesis, ETH Zürich Diss. ETH No. 21562, 2013, http://dx.doi.org/10.3929/ethz-a-010144564.
[5] O. Zimmer, Phys. Lett. B 685 (2010) 38, http://dx.doi.org/10.1016/j.physletb.2010.01.046.
[6] A.P. Serebrov, O. Zimmer, P. Geltenbort, et al., JETP Lett. 91 (2010) 6, http://dx.doi.org/10.1134/S0021364010010029.
[7] M. Pospelov, A. Ritz, Ann. Phys. 318 (2005) 119, http://dx.doi.org/10.1016/j.aop.2005.04.002.
[8] R.D. Peccei, H.R. Quinn, Phys. Rev. Lett. 38 (1977) 1440, http://dx.doi.org/10.1103/PhysRevD.16.1791.
[9] F. Wilczek, Phys. Rev. Lett. 40 (1978) 279, http://dx.doi.org/10.1103/PhysRevLetters.40.279.
[10] S. Weinberg, Phys. Rev. Lett. 40 (1978) 223, http://dx.doi.org/10.1103/PhysRevLetters.40.223.
[11] K.A. Olive, et al., Particle Data Group, Chin. Phys. C 38 (2014) 090001, http://dx.doi.org/10.1088/1674-1137/38/9/090001.
[12] J.E. Moody, F. Wilczek, Phys. Rev. D 30 (1984) 130, http://dx.doi.org/10.1103/PhysRevD.30.130.
[13] I. Antoniadis, S. Baeßler, M. Büchner, et al., C. R. Phys. 12 (2011) 755, http://dx.doi.org/10.1016/j.crhy.2011.05.004.
[14] J. Jaeckel, A. Ringwald, Annu. Rev. Nucl. Part. Sci. 60 (2010) 405, http://dx.doi.org/10.1146/annurev.nucl.012809.104433.
[15] K. Baker, G. Cantatore, S.A. Cetin, et al., Ann. Phys. 525 (2013) A93, http://dx.doi.org/10.1002/andp.201300727.
[16] S. Mantry, M. Pitschmann, M.J. Ramsey-Musolf, Phys. Rev. D 90 (2014) 054016, http://dx.doi.org/10.1103/PhysRevD.90.0540.
[17] M. Arik, S. Aune, K. Barth, et al., Phys. Rev. Lett. 107 (2011) 261302, http://dx.doi.org/10.1103/PhysRevLett.107.261302.
[18] F. Atchinson, B. Blau, M. Daum, et al., Phys. Rev. C 74 (2006) 055501, http://dx.doi.org/10.1103/PhysRevC.74.055501.
[19] K. Bodek, M. Daum, R. Henneck, et al., Nucl. Instrum. Methods A 597 (2008), http://dx.doi.org/10.1016/j.nima.2008.09.018.
[20] C.A. Baker, Y. Chibane, M. Chouder, et al., Nucl. Instrum. Methods A 736 (2014), http://dx.doi.org/10.1016/j.nima.2013.10.005.
[21] S. Afach, G. Bison, K. Bodek, et al., J. Appl. Phys. 116 (2014) 084510, http://dx.doi.org/10.1063/1.4894158.
[22] P. Knowles, G. Bison, N. Castagna, et al., Nucl. Instrum. Methods A 611 (2009) 306, http://dx.doi.org/10.1016/j.nima.2009.07.079.
[23] P.J. Mohr, B.N. Taylor, D.B. Newell, Rev. Mod. Phys. 84 (2012) 1527, http://dx.doi.org/10.1103/RevModPhys.84.1527.
[24] M. Fertl, PhD thesis, ETH Zürich Diss. ETH No. 21638, 2013, http://dx.doi.org/10.3929/ethz-a-010049897.
[25] T. Schmidt, Z. Phys. Hadrons Nucl. 106 (1937) 358, http://dx.doi.org/10.1007/BF01338744.
[26] K. Tullney, F. Allmendinger, M. Burghoff, et al., Phys. Rev. Lett. 111 (2013) 100801, http://dx.doi.org/10.1103/PhysRevLetters.111.100801.

[27] M. Bulatowicz, R. Griffith, M. Larsen, et al., Phys. Rev. Lett. 111 (2013) 102001, http://dx.doi.org/10.1103/PhysRevLetters.111.102001.
[28] P.-H. Chu, A. Dennis, C. Fu, et al., Phys. Rev. D 87 (2013) 011105, http://dx.doi.org/10.1103/PhysRevD.87.011105.
[29] A.K. Petukhov, G. Pignol, D. Jullien, et al., Phys. Rev. Lett. 105 (2010) 170401, http://dx.doi.org/10.1103/PhysRevLetters.105.170401.
[30] V.V. Voronin, V.V. Fedorov, I.A. Kuznetsov, JETP Lett. 90 (2009) 5, http://dx.doi.org/10.1134/S0021364009130025.
[31] T. Jenke, G. Cronenberg, J. Burgdörfer, et al., Phys. Rev. Lett. 112 (2014) 151105, http://dx.doi.org/10.1103/PhysRevLetters.112.151105.
[32] A.P. Serebrov, Phys. Lett. B 680 (2009) 423, http://dx.doi.org/10.1016/j.physletb.2009.09.025.
[33] G. Raffelt, Phys. Rev. D 86 (2012) 015001, http://dx.doi.org/10.1103/PhysRevD.86.015001.
[34] A. Arvanitaki, A.A. Geraci, Phys. Rev. Lett. 113 (2014) 161801, http://dx.doi.org/10.1103/PhysRevLett.113.161801.